Search for Heavy Z' Bosons in the Dielectron Channel with 200 pb^{-1} of Data with the DØ Detector

The DØ Collaboration

URL: http://www-d0.fnal.gov

We report preliminary results on a search for a heavy partner of the Z boson with Standard-Model-like couplings to fermions in the dielectron channel using $\sim$ 200 pb^{-1} of data collected in Run II of the Fermilab Tevatron. We set a new lower limit on the mass of the Z' boson with the SM-like couplings to fermions of 780 GeV at the 95% confidence level, which is the stringest limit from direct searches to date. We also set the most stringent direct limits on the Z' mass in the variety of E_6 GUT-inspired models.

Preliminary Results for Winter 2004 Conferences

I. Z' MODELS

A heavy partner of the Z boson, a so-called Z' boson, is found in multiple extensions of the Standard Model (SM). It is particularly popular in extended technicolor models, grand unified theories, models with extra dimensions, and little Higgs models. Depending on the model, couplings of the Z' boson to light fermions could be either SM-like or modified. In some models, Z' couples only to the third generation fermions. A good review of the various extended gauge theory models and references can be found in Ref. [1].

One of the simplest extensions is the *Left-Right Symmetric Model (LRM)* where a right-handed gauge group is added to the electroweak sector restoring parity at high-energy and giving $SU(2)_R \times SU(2)_L \times U(1)$ [2]. The LRM also falls out naturally as a subgroup of $SO(10)$ and an alternative LRM from E_6 models, both favored in grand unified theories [3]. Superstring theories also give rise to E_6 as the simplest unifying group with a slightly modified $U(1)$ generator for the Z'.

This analysis considers a Z' resonance with SM-like coupling to all generations of matter. Although there is no theoretical model for such a Z' boson as it is non-gauge invariant, this reference model is very useful for experimental comparisons [1]. The width of such a Z' boson is proportional to the Z' mass, once all the decay channels are open. The best published direct lower limit on such a Z' boson comes from the CDF experiment in the Tevatron Run I [4], and is 690 GeV at the 95% confidence level (CL). The published DØ Run I limit [5] is 670 GeV.

We extend the comparison of the experimental results to Z' models inspired by GUT $SO(10)$ and E_6 models using the conventions of Ref. [6] and Ref. [7] as followed by CDF for their results presented in 2003-2004. E_6 can break down to:

$$E_6 \rightarrow SO(10) \times U(1)_\phi \rightarrow SU(5) \times U(1)_\chi \times U(1)_\phi \rightarrow SU(3) \times SU(2) \times U(1)_Y \times U(1)_\chi \times U(1)_\phi \qquad (1)$$

In this general case, there are two additional neutral vector bosons and the physical state can be expressed as a linear combination i.e.

$$Z'(\theta) = Z_\psi \cos\theta + Z_\chi \sin\theta \qquad (2)$$

Here θ is a continuous parameter characterizing the theory and can range between 0 and 2π radians. The four models commonly considered in the references above are Z_ψ, Z_η, Z_χ and Z_I, which correspond to θ values of 0, $\arctan(\sqrt{3/5})$, $\pi/2$ and $\arctan(-\sqrt{5/3})$ radians respectively.

II. INTRODUCTION

This analysis is a straightforward extension of the search for TeV^{-1} extra dimensions in the dielectron channel, described in detail in Ref. [8]. The data, background, efficiencies, and systematic errors are the same as in the former analysis. The extraction of limits on the Z' boson is based solely on the dielectron mass spectrum, shown in Fig. 1. Since the fraction of instrumental background is similar in the two topologies studied, where both electrons are in the central calorimeter cryostat (CC-CC) or one electron is in the central cryostat and one is in the end-cap cryostat (CC-EC), for the purpose of this search we combine spectra for these two topologies rather than performing a more involved, Bayesian fit for each topology and then combining the results by combining the likelihoods.

The results of this search can be easily reinterpreted as a search for *any* heavy narrow resonance decaying into $e^+ e^-$ pairs. Examples of such resonances include technirho and techniomega particles found in technicolor models, Randall-Sundrum gravitons, etc.

III. SEARCH FOR A SM-LIKE Z' BOSON IN THE DIELECTRON CHANNEL

A. Data Selection

Data selection for this analysis is detailed in Ref. [8]. It corresponds to $\approx 200 \ \mathrm{pb}^{-1}$ of data collected by the DØ experiment in Run II of the Fermilab Tevatron in 2002-2003. The overall efficiency of the event selection are as follows [8]:

$$\varepsilon_{\mathrm{CC-CC}} = 0.74 \pm 0.02;$$
$$\varepsilon_{\mathrm{CC-EC}} = 0.74 \pm 0.02; \qquad (3)$$
$$(4)$$

The analysis sample consists of 14,195 events, corresponding to 8,246 CC-CC and 5,949 CC-EC combinations. The event selection flow is detailed in Ref. [8].

The integrated luminosity on this sample is known with 6.5% instrumental error. In order to decrease the dependence on the luminosity measurement, we normalize all the cross sections to the NNLO Z production cross section, known well theoretically [9].

B. Backgrounds

The QCD background is estimated via the method of Ref. [8]. The Drell-Yan background is simulated with the main signal Monte Carlo. Since the direct diphoton production is at least an order of magnitude less than Drell-Yan production even at high masses, background from direct diphotons with photon conversions is negligible. All other physics backgrounds that result in dielectron final state are negligible.

C. Systematics

We consider various sources of systematic uncertainties for signal and background, which are documented in Table I. Note that many sources of systematics are cancelled in the ratio of the Z and Z' cross sections. The remaining uncertainties include a mass-dependent K-factor uncertainty of 10%, E_T/η dependence of the efficiency of 7%, and signal acceptance uncertainty of 5%.

Source of signal systematics	Uncertainty
K-factor uncertainty	10%
E_T and eta dependence of the efficiency	7%
Signal acceptance uncertainty	5%
Total	13%
QCD background uncertainty	10%
DY background uncertainty	10%

TABLE I: Sources of systematic uncertainty on the calculated differential cross section.

The QCD background uncertainty stems from the uncertainty on normalization at low masses, which is slightly less than 10%; the DY background uncertainty mainly stem from the fact that we conservatively use a flat K-factor for DY, which results in 10% uncertainty due to the mass-dependence of the K-factor.

D. Optimum Window

As seen from Fig. 1, the background at high masses drops exponentially, with a slope of -0.0119 GeV^{-1}. Mass windows for the counting experiment for low mass points have been optimized using previously established analytic techniques [10] to enhance the Gaussian significance, i.e. $S/\sqrt{B}$, given the exponential background. For the Z' masses above 500 GeV, where the background is small, we used fixed $\pm 3\sigma$ mass windows, centered on the resonance position, where σ is the RMS of the reconstructed Z' peak.

The width of the Z' boson has been obtained using a fast detector simulation and is shown in Fig. 2. For the Z' masses below ~ 600 GeV, the width is dominated by the detector resolution and grows roughly linearly with mass. For a higher mass Z', the internal width is comparable to the resolution, so the dependence on the mass changes.

The results of the counting experiments in each mass window are summarized in Table II.

Since the data in each window are consistent with the expected background, we proceed with setting limits on the existence of the Z' resonance.

E. Acceptance Calculation

The acceptance and cross-section for Z'-bosons production with SM-couplings was calculated using Pythia 6.202 [11] with CTEQ5L pdf's and the DØ parametrized fast detector simulation for electron smearing based on the measured calorimeter resolution for electromagnetic objects. No geometrical fiducial cuts are applied. Masses from 200–800 GeV were generated with only the Z' production turned on at the generator level and Z' decays to electron pairs.
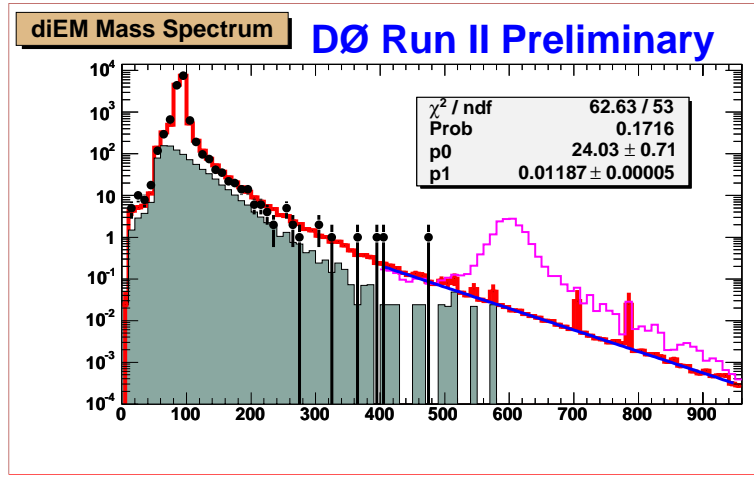
FIG. 1: Dielectron mass distribution. Points: data; shaded region: QCD background; open histogram: sum of the Drell-Yan and QCD background. Also shown: fit of the background at high masses to an exponent (blue solid line) and a shape of the Z' signal for the Z' mass of 600 GeV (magenta histogram). The fit parameter $p1$ corresponds to the (negative) slope of the exponent, while $p0$ reflects the normalization.
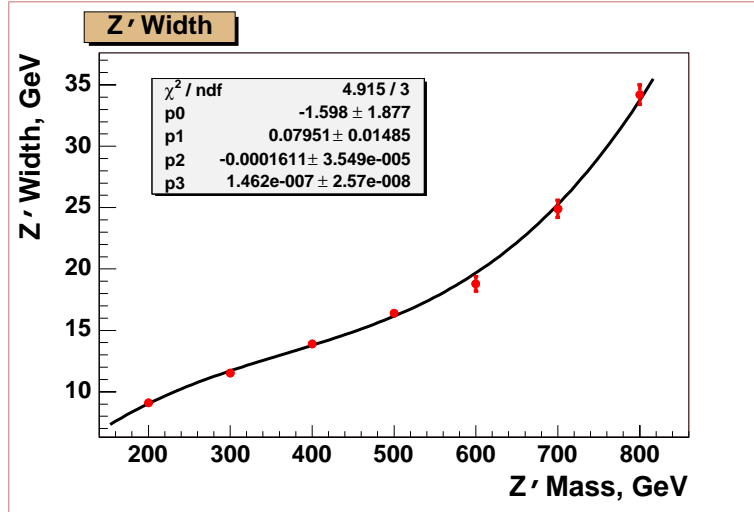

FIG. 2: Reconstructed width of the Z' resonance, as a function of its mass. Based on fast simulation and Z' with the SM-like couplings to fermions.

Simulated events were accepted if two electrons had $p_T > 25$ GeV/c at the generator level and were in the fiducial pseudorapidity range of $|\eta| < 1.1$ (CC) or $1.5 < |\eta| < 2.4$ (EC), with only CC-CC and CC-EC combinations being accepted. The invariant mass was calculated from the simulated electrons and the mass window cut of Table II was applied. The generated cross-section for $Z' \to ee$ and acceptance for CC-CC, CC-EC and total are shown in Table III. The mass window cut is about 80% efficient at the higher masses (see table). Events become much more central as expected for the higher Z' masses.

In PYTHIA simulation it has been assumen that the width of the Z is proportional to its mass. This ignores WW and $t\bar{t}$ channels opening at high masses, but their effect on the internal width is small. The branching fraction to electrons is calculated by PYTHIA and reflects opening of new channels.

Systematic uncertainties were estimated on the acceptance for contributions from Drell-Yan (DY) inteference and for the mass window cut. Events were generated with and without DY inteference in Pythia for a Z' mass of 500 GeV and the acceptance reduces by 2% due to the mass window cut. Varying the mass window by $\pm 1\sigma$ of the Z' width uncertainty at the higher simulated masses changes the acceptance by 1.5%. The statistical uncertainty is about 1% based on 10,000 event samples. A conservative overall 5% uncertainty is chosen to cover mass dependence of the pdf's.

TABLE II: Optimum window sizes and the results of the counting experiment in these windows.

Z' Mass	Window	DY bck.	QCD bck.	Total bck.	Bck. Err	Data
200 GeV	190–210 GeV	13.0	15.6	28.6	2.9	32
300 GeV	280–320 GeV	1.6	4.3	5.9	0.59	3
400 GeV	380–420 GeV	0.14	1.05	1.19	0.12	2
500 GeV	450–550 GeV	0.16	0.70	0.86	0.09	1
600 GeV	540–660 GeV	0.05	0.26	0.31	0.03	0
700 GeV	620–780 GeV	0.05	0.11	0.16	0.02	0
800 GeV	700–900 GeV	0.05	0.05	0.09	0.01	0

TABLE III: Leading order production cross-section and acceptances for $Z' \rightarrow ee$ (from PYTHIA). Only statistical uncertainties are shown.

Z' Mass	$\sigma(Z') \times B(Z' \rightarrow ee)$	K-factor $(K(M))$	$\sigma(Z' \rightarrow ee)K(M)/ \sigma(Z \rightarrow ee)K(M_Z)$	Acceptance CC-CC	Acceptance CC-EC	Acceptance Total	Window cut efficiency
200 GeV	15.6 pb	1.20	8.66×10^{-2}	0.236 ± 0.004	0.173 ± 0.004	0.409 ± 0.005	0.717
300 GeV	3.67 pb	1.24	2.10×10^{-2}	0.327 ± 0.005	0.157 ± 0.004	0.484 ± 0.005	0.810
400 GeV	1.17 pb	1.27	6.87×10^{-3}	0.330 ± 0.005	0.114 ± 0.003	0.444 ± 0.005	0.708
500 GeV	0.409 pb	1.31	2.48×10^{-3}	0.440 ± 0.005	0.110 ± 0.003	0.550 ± 0.005	0.868
600 GeV	0.155 pb	1.35	9.68×10^{-4}	0.446 ± 0.005	0.087 ± 0.003	0.533 ± 0.005	0.841
700 GeV	0.0591 pb	1.40	3.83×10^{-4}	0.457 ± 0.005	0.064 ± 0.002	0.521 ± 0.005	0.825
800 GeV	0.0235 pb	1.46	1.59×10^{-4}	0.451 ± 0.005	0.052 ± 0.002	0.503 ± 0.005	0.785

Since signal simulation is done at the leading order (LO), we normalize all the cross sections to the Z production cross section of 181.1 pb, as given by PYTHIA. The normalization is done after multiplication of the LO cross sections by the mass-dependent K-factor of Ref. [9], which has the value of 1.194 at the Z mass and grows slowly at high masses. The K-factor and the cross section ratios are shown in Table III.

F.   Limits on the Z' cross section

In order to set the limits on the Z'/Z cross section ratio, we set the upper 95% CL limits on the cross section ratio based on the counting experiment in each window. In order to do that we need to measure the effective integrated luminosity in our sample. We do this *in situ*, using the central value of the NNLO $Z(ee)$ cross section of 252 ± 9 pb [9].

For the limit setting we decouple the acceptance (A) calculations from the limit setting procedure and set the limits on $\sigma(Z') \times B(Z' \rightarrow ee) \times A$. The advantage of this method is that only the experimental component, i.e. the dielectron selection efficiency is taken into account, and thus the limits can be interpreted as limits on any heavy particle decaying into dielectrons. While a particular width of the resonance has been assumed when optimizing the window used in the analysis, the result applies for any resonance, as the window-cut acceptance can be easily recalculated. The optimization won't be as precise as for the Z', but since the significance only varies very slowly with the size of the window, it is still expected to be fairly close to the optimum. Particularly, one can use the calculated Z' acceptance as a conservative estimate for *any narrow resonance* decaying into dielectrons, e.g. technirho or techniomega. Our limits can then be reinterpreted in a straightforward manner for a variety of models without knowing the details of the DØ apparatus or the analysis.

A standard Bayesian limit-setting procedure with the signal and background systematics discussed above is applied. The results are listed in Table IV and shown in Fig. 3. The lower limit on the SM-like Z' mass obtained in this analysis is 780 GeV at the 95% CL. Note, that if one uses a constant K-factor, instead of the mass-dependent one, the limit is shifted down by only 5 GeV, which gives an estimate of the robustness of this analysis.

We also set the limits on Z' mass in a variety of E_6-type models, assuming the same acceptance and K-factor as for the SM-like Z'. The LO PYTHIA cross sections for Z' in these models, using the CTEQ5L pdf's, are listed in Table VI. They have been normalized to the LO Z cross section via the same procedure as was used for the SM-like Z', and compared with the experimental limits on the cross section ratio. The limits are summarized in Table IV and shown in Fig. 3.

TABLE IV: Upper 95% CL limits on $\sigma(Z' \to ee) \times A \times \varepsilon/sigma(Z \to ee)_{\mathrm{NNLO}}$ as a function of the Z' mass. The last column is obtained from the limit on the ratio by multiplying it by the cental value of the Z NNLO cross section of 252 pb.

Z' Mass	Total bck.	Bck. Err	Data	Ratio Limit	NNLO Limit
200 GeV	28.6	2.9	32	3.13×10^{-4}	79 fb
300 GeV	5.9	0.59	3	1.41×10^{-4}	35 fb
400 GeV	1.19	0.12	2	1.66×10^{-4}	42 fb
500 GeV	0.43	0.04	0	1.31×10^{-4}	33 fb
600 GeV	0.11	0.01	0	9.37×10^{-5}	24 fb
700 GeV	0.07	0.01	0	9.37×10^{-5}	24 fb
800 GeV	0.04	0.00	0	9.37×10^{-5}	24 fb

TABLE V: Leading order cross sections for the four reference $E-6$ Z' models: ψ, χ, η, and I. CTEQ5L pdf set has been used in the simulations.

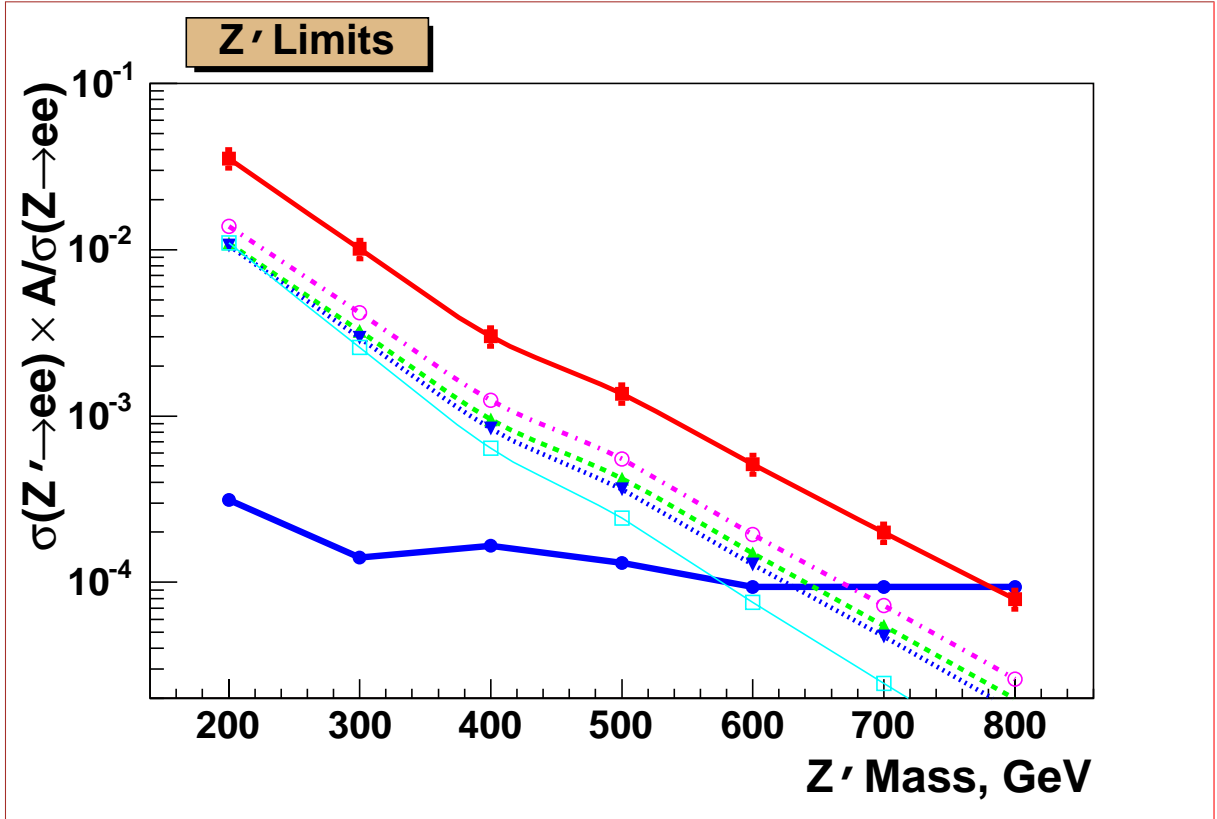| Z' Mass	$\sigma(Z'_\psi \to ee)$	$\sigma(Z'_\chi \to ee)$	$\sigma(Z'_\eta \to ee)$	$\sigma(Z'_I \to ee)$
200 GeV	4.79 pb	4.64 pb	6.06 pb	4.84 pb
300 GeV	1.18 pb	1.07 pb	1.52 pb	0.939 pb
400 GeV	0.369 pb	0.324 pb	0.481 pb	0.248 pb
500 GeV	0.127 pb	0.109 pb	0.166 pb	0.0732 pb
600 GeV	0.0452 pb	0.0386 pb	0.0586 pb	0.0229 pb
700 GeV	0.0163 pb	0.0140 pb	0.0215 pb	0.00732 pb
800 GeV	0.00588 pb	0.00497 pb	0.00775 pb	0.00242 pb

FIG. 3: Lower thick solid (blue) curve: upper 95% CL cross section times acceptance limits on production of the $Z'(ee)$. Other lines correspond to cross section times acceptance for the Z' in several models. The thick solid (red) curve: Z' with the SM-like couplings to fermions; dashed (green) curve: Z' in E_6 ψ model; dotted (blue) curve: Z' in E_6 χ model; dash-dotted (magenta) curve: Z' in E_6 η model; and thin solid (cyan) curve: Z' in E_6 I model.

TABLE VI: Lower 95% CL limits on the Z' mass in several extensions of the SM.

Model	Mass limit
SM-like couplings	780 GeV
ψ model	650 GeV
χ model	640 GeV
η model	680 GeV
I model	575 GeV

IV. CONCLUSIONS

We performed a search for heavy resonances decaying into the dielectron channel using ~ 200 pb^{-1} of data collected by the DØ Experiment at the Fermilab Tevatron in 2002-2003 (Run II). The data are in excellent agreement with Drell-Yan production and do not exhibit any evidence for new physics beyond the Standard Model, so we use them to set limits on the existence of the Z' boson. A lower limit on its mass has been set at 780 GeV at the 95% CL, assuming SM-like couplings to fermions. Lower limits have been also set on the Z' boson present in four popular extensions of the E_6 GUT theory. These are the most stringent direct limits on the Z' boson to date.

Acknowledgments

[1] M. Cvetic and S. Godfrey, hep-ph/9504216, 1995.
[2] J.C. Pati and A. Salam, *Phys. Rev. Lett.* **31**, 661 (1973); R.N. Mohapatra, *Phys. Rev.* **D11**, 2558 (1975); G. Sejanovic and R.N. Mohapatra, *Phys. Rev.* **D12**, 1502 (1975).
[3] J.L. Hewett and T.G. Rizzo, *Phys. Rep.* **183**, 193 (1989).; R.N. Mohapatra, *Unification and Supersymmetry*, Springer, 1992.; E. Ma, *Phys. Rev.* **D36**, 274 (1987).; K.S. Babu *et al*, *Phys. Rev.* **D36**, 878 (1987).
[4] CDF Collaboration, F. Abe *et al.*, Phys. Rev. Lett. **79**, 2192 (1997).
[5] DØ Collaboration, V.M. Abazov *et al.*, Phys. Rev. Lett. **87**, 061802 (2001).
[6] F. Del Aguila, M. Quiros and F. Zwirner, Nucl Phys. **B287**, 419 (1987).
[7] D. London and J.L. Rosner, Phys. Rev. **D34**, 5, 1530 (1986).
[8] DØ Collaboration, DØ Note 4349-Conf (2004),
   http://www-d0.fnal.gov/Run2Physics/WWW/results/NP/NP02.pdf.
[9] R. Hamberg, W.L. Van Neerven, and T. Matsura, Nucl. Phys. B**359**, 343 (1991).
[10] G. Landsberg and K.T. Matchev, Phys. Rev. D **62**, 035004 (2000).
[11] T. Sjostrand, P. Eden, C. Friberg, L. Lonnblad, G. Miu, S. Mrenna, and E. Norrbin, Comp. Phys. Comm. **135**, 238 (2001).